THREE-DIMENSIONAL MODEL FOR WOOD-POLE–STRENGTH PREDICTIONS

By Nilson Franco[1] and Patrick J. Pellicane,[2] Associate Member, ASCE

ABSTRACT: A three-dimensional finite element model was developed to predict the strength and failure location of nine wood transmission poles made from three commonly used North American species. All poles were 1,524–1,829 cm (50–60 ft) long, and were tested to failure as cantilever beams. The analysis methodology involved considering several 45.7-cm- (18-in.-) long segments, located along the pole length, that contained the most severe inherent characteristics. Each segment was analyzed recognizing actual material properties and appropriate boundary conditions. Important material properties for each segment were determined by measuring clear-wood elastic and strength parameters in undamaged sections taken from tested poles. The flow-grain model was used to describe the grain deviation around knots. For the nine poles studied, predicted and experimental strength values differed on average by 7%. The correct location was predicted in six of the nine poles studied. Where failure location was not predicted correctly, the failure was due to some pole characteristic not perceptible from a surface inspection.

INTRODUCTION

Specifications for distribution, telephone, and transmission poles are designed to ensure that these structures demonstrate adequate strength and can resist the service loads imposed on them during their life. The traditional method of estimating wood-pole properties follows the strength of materials procedures, and uses small, clear specimen test values for wood strength (Wood and Markwardt 1965). Although these procedures have been used throughout the world for decades, the availability of data from tests on full-size pole members has facilitated the development of predictive models based on contemporary statistical procedures (Goodman et al. 1981; Pellicane 1983, 1984, 1992). Statistical analyses, which provide rational estimates of pole-strength distributions, coupled with reliability analysis provide the basis for a probabilistic approach to wood pole design.

Clearly, the development of a data bank of strength values from tests of full-size distribution and transmission poles is time- and cost-intensive. This problem is further magnified in tropical countries such as Brazil, where there are many more species potentially usable in pole structural applications. The use of computer models to predict the mechanical behavior of large members and systems has long been recognized as a more cost-, labor-, and time-effective alternative to full-size testing. The availability of rational computer models to predict mechanical behavior of wood poles under load can obviate the need for extensive testing and help create grading rules that reflect structural performance. Recognizing the numerous benefits of computer experimentation over physical testing, this study focused on

[1]Res. Engr., Instituto de Pesquisas Tecnologicas do Estado de São Paulo, Wood Div., São Paulo, Brazil.

[2]Prof. of Wood Engrg., Dept. of Forest Sci., Colorado State Univ., Fort Collins, CO 80523.

Note. Discussion open until December 1, 1993. To extend the closing date one month, a written request must be filed with the ASCE Manager of Journals. The manuscript for this paper was submitted for review and possible publication on June 25, 1992. This paper is part of the *Journal of Structural Engineering*, Vol. 119, No. 7, July, 1993. ©ASCE, ISSN 0733-9445/93/0007-2199/$1.00 + $.15 per page. Paper No. 4183.

the development of a model to predict the strength of an individual pole and the associated failure location.

Objective

The objective of this study was to develop and verify a three-dimensional finite element model to predict the magnitude of the ultimate load, as well as the failure location for wood poles loaded as cantilever beams. The model accounts for the mechanical properties of the material and incorporates the effects of key pole characteristics (spiral grain, knots and their associated local grain deviations, and material inhomogeneity).

Literature Review

Theoretical Strength Prediction of Wood Members

It is well known that the strength of wood members is determined by a complex interaction of numerous material and geometric factors. The cylindrical shape of wood poles in no way simplifies the task of strength prediction. In recent years, considerable progress has been made to develop theoretical insights into the quantification of stress distributions in wood products.

Research performed over the past 15 years has increased our ability to predict stress distributions in wood members. Phillips et al. (1981) demonstrated that the grain pattern associated with a knot can be predicted by assuming the material to be a fluid subjected to laminar flow around an elliptical obstruction. The grain angle at any location near a knot can be predicted by the fundamental mathematical relationship for laminar flow given by Milne-Thompson (1950):

$$\psi = v(a + b)\sinh(\xi - \xi_0)\sin(\eta - \alpha) \quad \text{.........................} \quad (1)$$

where ψ = stream function (grain direction analogy); v = speed of flow (taken as unity in analogy); a, b = lengths of major and minor axes of elliptical flow obstacle; ξ, η = elliptical coordinates, around the flow obstacle at which the value of ψ is sought; α = angle of attack of flow (cross-grain angle for wood member in analogy); and ξ_0 = constant.

Dabholkar (1980) theoretically modeled the grain pattern associated with a knot using an interactive routine to solve (1), since no direct solution exists in elliptical coordinates. With this model as a descriptor of the fundamental geometry of wood, a finite element program was developed to predict the stress distribution in solid wood with knots and cross grain subjected to axial tension. Cramer and Goodman (1986) continued this work generalizing the capabilities of Dabholkar's program. The primary improvement related to accounting for partial edge knots. Cramer and McDonald (1989) further modified the program to include a more sophisticated fracture mechanics algorithm. Zandbergs and Smith (1988) introduced an additional refinement to Cramer's (1981) program that enabled the global cross grain to be modeled.

Pole-Strength Prediction

There has been a long standing interest in predicting the strength of structural wood members from both probabilistic and deterministic fashions. Work by Johnson and Galligan (1983), Pellicane (1983, 1984, 1985, 1993), and Tichy (1983) have contributed much toward the prediction of the probability distribution of wood-member strength. However, much interest remains in the deterministic strength of wood products.

Loaded members containing knots may fail at stresses that are a fraction of clear wood strength. Bodig (1986) studied the influence of knots in pole structures and analyzed the modulus of rupture (MOR) at the ground line of new, green, untreated, 1,219-cm- (40-ft-) long Douglas fir poles, as a function of maximum knot diameter and sum of knot diameters in a 30.5-cm (1-ft) section. The results showed that the effect of a single knot is not highly significant, but the tendency of decreasing strength with increasing maximum knot diameter was observed. A similar tendency was observed when the maximum sum of knot diameters in a 30.5-cm (1-ft) section increased. Concerning failure location, little correlation was observed between the location of the maximum sum of knots and the rupture point. The conclusion reached was that the maximum sum of knots did not predict the failure location (Bodig 1986).

A model involving the net moment of inertia (i.e., the moment of inertia of the section without the triangular area of the knots) was studied by Dashiell (1985). The principal conclusion of his study was that this technique lacked the sensitivity to predict pole strength accurately. Wang (1987) an-

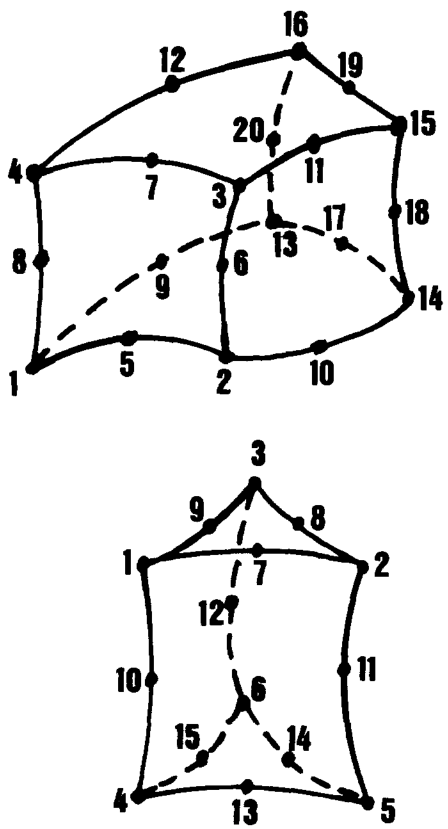

FIG. 1. Schematic Representations of 20-Node Parallelepiped (IPQS) and 15-Node Wedge (WEDGE15) Finite Elements

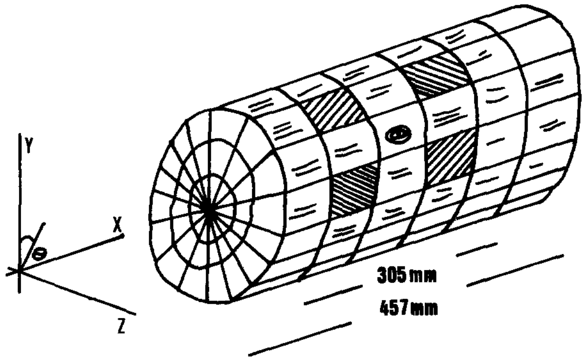

FIG. 2. Finite Element Mesh to Represent Pole Section of 45.7 cm (18 in.) Long

alytically studied, in two-dimensional analysis, the interaction between knots by applying the principle of superposition to define the least distance at which two knots have an appreciable interactive effect. His results indicated that a 2-D model lacked the ability to accurately represent the complexities associated with strength prediction of a 3-D pole structure. In addition, he concluded that even empirical methods accounting for multiple wood characteristics were better than the 2-D numerical model based on only knot-related parameters. Clearly, no rational vehicle currently exists to predict pole strength.

Mathematical Model for Wood Poles

Finite Element Model

For stress analysis of continuum problems, the computer program Georgia Tech Structural Design Language (GTSTRUDL), version 8701 CDC (*GTSTRUDL* 1985), was used. GTSTRUDL is a computer program capable of performing a linear elastic stress analysis using a variety of contemporary elements. Parallelepiped and wedge elements (Fig. 1) were selected with aspect ratios approaching unity. Although these linear-strain elements had the geometry that ensured mathematical stability, the number of equations generated in the analysis far exceeded the capacity of most mainframe computers. To reduce the amount of computer resources needed in this study for each pole, all locations in which the number of knots and their angular position with respect to the neutral plane were considered to impact the stress distribution in the pole severely were selected for mathematical analysis.

Multiple knots are commonly referred to in standards as the sum of knots in any 30.5-cm (1-ft) segment. Hence, any 30.5-cm (12-in.) length was mathematically idealized as four disks of 7.6-cm (3-in.) elements. To avoid difficulties created by load and boundary effects on the 30.5-cm (1-ft) segment, two more disks were added to the segment (one on each end). These disks serve as transition disks or elements. Fig. 2 shows the 3-D finite element segment mesh to represent any section along the pole. Each pole segment was analyzed as an 45.7-cm- (18-in.-) long section with the appropriate boundary conditions (Fig. 2).

The poles were analyzed as statically determinant cantilever beams with a concentrated load applied 61.0 cm (2 ft) from the pole tip. Thus, at any

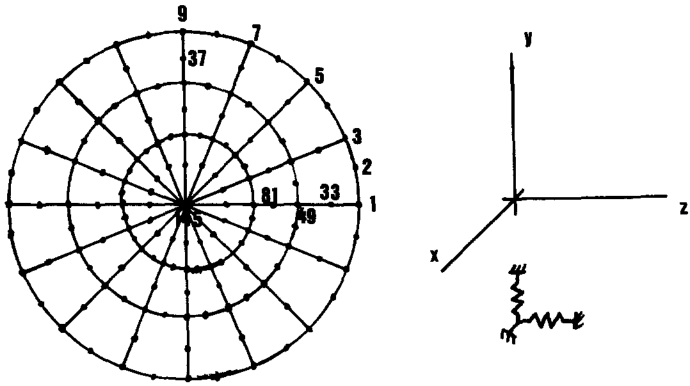

FIG. 3. Nodal Arrangement on Pole Cross Section with Spring Boundary Conditions

section, the bending moment and shear force can be easily evaluated. The stresses developed by the applied forces were evaluated and appropriately distributed to each of the 145 nodes (see Fig. 3) located at the far section (closer to the pole tip). At the near section (closer to the butt), a set of two mutually orthogonal springs was attached to each node to permit movement in the y- and z-directions (see Fig. 3). The mesh pattern for the pole segment as shown in Fig. 1 is a function of the pole segment diameter only. The GTSTRUDL program generates the mesh using the pole radius and the radial increment as input to the process.

Modeling Grain Deviation around Knots

A method to model the effects of knots and associated grain deviation in the poles was developed in this study. To represent a knot and the associated grain deviation, knots were modeled as cones, with the vertex located at the pith (geometric center) and perpendicular to the longitudinal direction of the pole. Grain deviation around a knot was assigned to the four elements most affected by the presence of a knot (Fig. 2), depending on the knot diameter obtained from the flow-grain analogy. When multiple knots were present in the same segment (knot cluster), the superposition effect for grain deviation was adopted as shown schematically in Fig. 4. Whenever a knot occurred in the outer surface, three elements were affected (one in each layer). Since knots in dry wood tend to check and create discontinuities in the material, they are considered incapable of transmitting tension. Therefore, no consideration of knot properties was made. The effect of the knot on the element stiffness was taken into account by decreasing the modulus of elasticity (E_L) and, consequently, the element stiffness matrix, by the ratio of the net width (element width minus the knot diameter) to element width.

The flow-grain analogy model [(1)] was used to determine the grain angles around the knots and the maximum average grain-angle deviation in the stream lines (associated with knot diameters varying from 1.9 to 7.6 cm [0.75 to 3.0 in.]) to be evaluated. The average maximum fiber deviation angle was 54.5°.

From data generated by the flow-grain analogy program, the grain deviation caused by a 5.1-cm (2.0-in.) knot was 54.5°. To represent the grain deviation angles for smaller knots in the elements of the model, a function was developed which correlates the area influenced by the presence and diameter of a knot. Fig. 5 illustrates the area affected by a 3.81-cm- (1.5-in.-) diameter knot in western red cedar using the mesh and angles predicted by the flow-grain analogy. The knot segment is located in the lower right corner of Fig. 5.

Using the flow-grain analogy, the areas affected by the presence of a knot were evaluated for knots 1.27, 2.54, 3.81, and 5.08 cm (0.5, 1.0, 1.5, and 2.0 in.) for Douglas fir and western red cedar, and are given in Table 1. The curve indicated in Fig. 6 represents a function relating the knot diameter and the area affected by the presence of a knot.

The ratio between the influence area of a knot less than 5.08 cm (2.0 in.) to one 5.08 cm (2.0 in.) in diameter was taken as the coefficient to represent the decreasing factor over the maximum deviation angle. The following function, which incorporates the decreasing factor, was used to evaluate the deviation angle for knots less than 5.08 cm (2.0 in.) in diameter:

$$\alpha_d = \frac{A_d}{A_{2''}} \cdot \alpha_{\max} = \frac{A_d}{A_{2''}} \cdot 54.5^\circ = K \cdot 54.5^\circ \quad \text{(2)}$$

The coefficient K was evaluated in increments of 0.25 cm (0.1 in.) according to the function in (2). Table 2 includes the deviation angle for these knots.

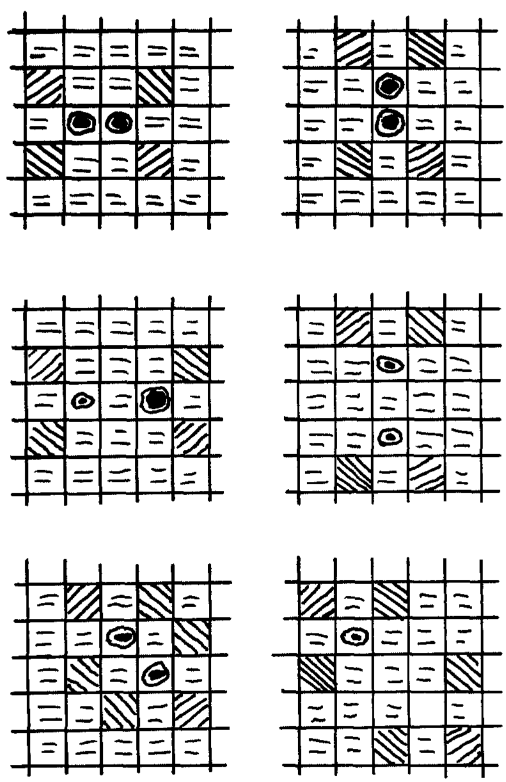

FIG. 4. Geometrical Idealization of Knot Clusters

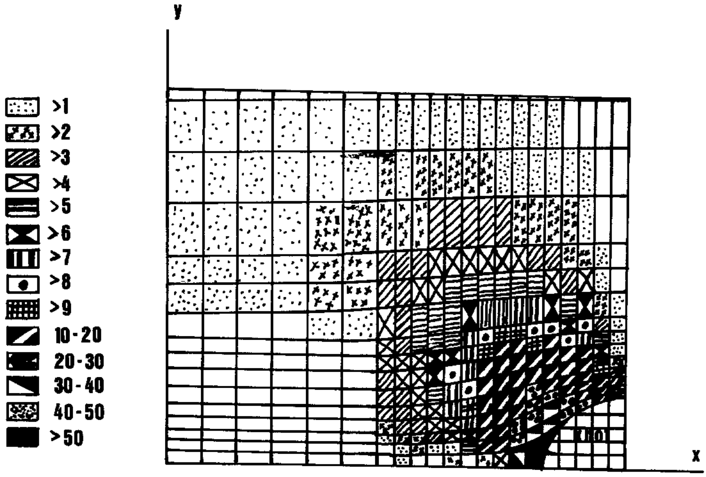

FIG. 5. Flow-Grain Pattern for 3.81-cm- (1.5-in.) Diameter Knot in Western Red Cedar and Associated Fiber Deviation (Degrees)

TABLE 1. Area (Evaluated in One-Quarter of Mesh) Affected by Presence of Knot, Using Flow-Grain Analogy

Knot diameter (mm) (1)	Area (mm^2) Western red cedar (2)	Douglas fir (3)
12.7	465	471
25.4	1,845	1,768
38.1	4,297	4,471
50.8	7,110	7,110

Using the parallelepiped and wedge-shaped element types available in GTSTRUDL as well as the parameters defined previously (e.g., the number of disks in a segment and number of elements in a disk), the segment idealized to model the pole behavior was divided into 288 elements (Fig. 2). The element types, isoparametric quadratic solid (IPQS) (six-face, 20-node [joint] element) and Wedge15 (four-face, 15-node element) (Fig. 1), were selected for use from the GTSTRUDL library.

Material Characteristics and Data Collection

In this study, nine poles (three each of southern pine, Douglas fir, and western red cedar), ranging from 1,220 to 1,829 cm (40 to 60 ft) long, were mapped for knot location, spiral grain, and material variation with length and diameter; numerically analyzed; and tested to failure. To evaluate the mechanical properties of the clear wood, undamaged specimens were cut from tested poles. Bending tests on small-clear specimens were conducted to determine the necessary mechanical properties of the wood.

All measurements on the poles (profile, spiral grain, knot map, and moisture content) were taken before the poles were tested to failure in bending. Starting at the pole butt and continuing to the tip, the circumfer-

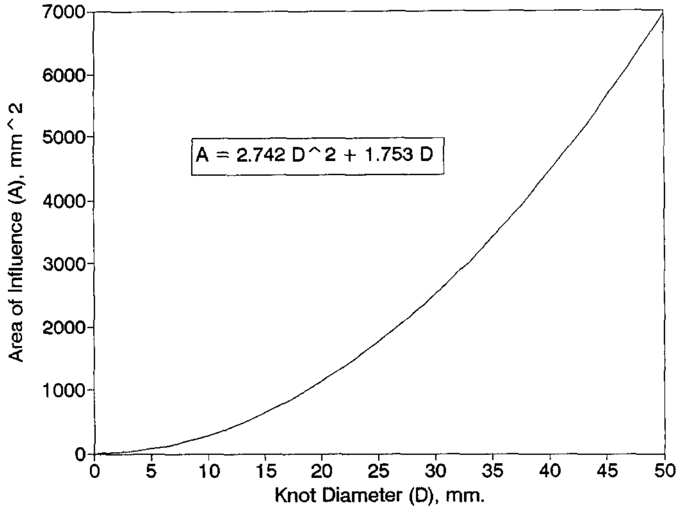

FIG. 6. Curve Fitted for Area of Influence (Angles of Deviation Less than or Equal to 2°) for Knots in Douglas Fir and Western Red Cedar Using Flow-Grain Analogy

TABLE 2. Effective Maximum Deviation Angle for Knot Diameters between 12.7 and 50.8 mm

Knot diameter (mm) (1)	Affected area (mm^2) (2)	$K = A1/A2$ (3)	Effective angle ($K \times 54.5°$) (4)
12.7	465	0.065	3.533
15.2	664	0.093	5.050
17.8	898	0.125	6.831
20.3	1,168	0.163	8.882
22.9	1,473	0.206	11.203
25.4	1,814	0.253	13.794
27.9	2,189	0.306	16.650
30.5	2,601	0.363	19.781
33.0	3,048	0.425	23.182
35.6	3,530	0.493	26.848
38.1	4,047	0.565	30.783
40.6	4,600	0.642	34.988
43.2	5,188	0.724	39.464
45.7	5,812	0.811	44.205
48.3	6,470	0.903	49.215
50.8	7,165	1.000	54.500

ence at each 91.4-cm (3-ft) interval was measured to the nearest 5.08 cm (0.1 in.). At the same 91.1-cm (3-ft) interval where the diameters were measured, grain deviation measurements were also made.

For each of the nine poles, the knot diameters were recorded, along with their longitudinal and circumferential locations along the pole. The knot map included all knots from the groundline to the tip with diameter greater than or equal to 1.27 cm (0.5 in.). After the measurements of circumfer-

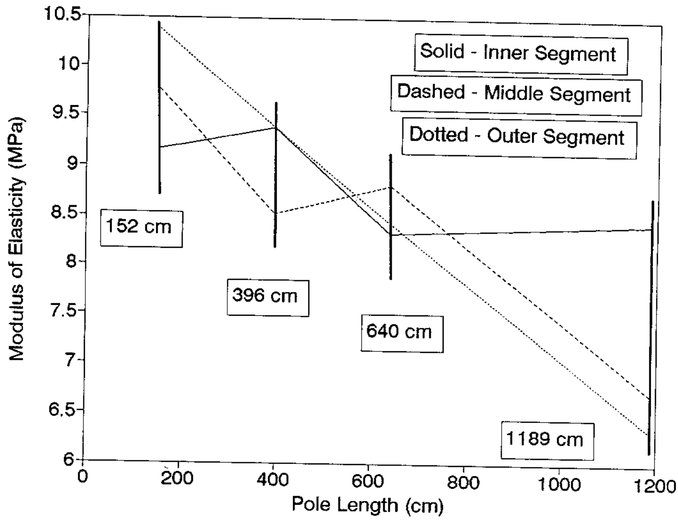

FIG. 7. Example of Variation in E_L along Southern Pine Pole Measured at Three Locations along Radius of Pole

ences, knots, and spiral grain were conducted, each pole was placed in the clamps of the testing apparatus and loaded as a cantilever beam until failure. After rupture, four 61.0-cm- (2-ft-) long undamaged segments were cut from each pole. These four locations were at 152, 396, 640, and 1,189 cm (5, 13, 21, and 39 ft) from the butt.

The material characteristics determined experimentally on logs cut from the poles included E_L and MOR parallel to grain. A minimum of 12 specimens per pole were prepared for bending tests (three per pole segment). On each segment, the three specimens were marked in the radial direction centered at each third of the radius. The bending specimens were 2.54 by 2.54 by 38.1 cm (1.0 by 1.0 by 15.0 in.). The objective of the bending test was to develop material data for input into GTSTRUDL. The E_L and MOR were determined according to ASTM (*Annual* 1988). Using the results obtained from small, clear specimens and assuming linear variation, the relationships between E_L and MOR with position along the poles were established. To build the curves to represent the wood MOR and E_L variation along each pole, four samples located between the ground line and the load application point were evaluated. The strength and stiffness values for intermediate points were obtained by linear interpolation (Fig. 7).

Nine elastic parameters (E_L, E_T, E_R, G_{LT}, G_{TR}, G_{LR}, ν_{LR}, ν_{LT}, and ν_{TR}) are necessary to build the element compliance matrix used in the 3-D finite element analysis. According to Bodig and Goodman (1973), all other elastic properties can be correlated to E_L. The equations presented in Bodig and Goodman (1973) were used to predict the other nonmeasured elastic parameters (E_R, E_T, G_{RT}, G_{TL}, and G_{RT}) for each species. The values of the Poisson's ratios were assumed constant.

Model Verification

Each 45.7-cm- (18-in.-) long pole segment was analyzed as a cylinder with a diameter equal to that found at the edge nearest the butt. Using the

TABLE 3. Summary of Maximum Stresses Developed on Pole Segments by Finite Element Analysis

Pole (1)	Section (2)	Near side (mm) (3)	Maximum stress (MPa) (4)	Joint (5)
(*a*) Western Red Cedar				
85	1	152	−11.2	547
85	2	3,581	−12.9	414
85	3	5,893	−15.2	934
85	4	6,731	12.0	539
88	1	660	−6.9	547
88	2	2,413	−8.4	934
88	3	3,886	−7.2	220
91	1	660	17.4	732
91	2	1,473	−18.6	546
91	3	2,413	17.0	293
(*b*) Douglas Fir				
162	1	864	20.0	732
162	2	1,499	−18.9	740
162	3	2,235	−19.1	740
174	1	0	−20.7	739
174	2	711	−22.9	605
174	3	1,626	−21.7	609
174	4	2,438	−21.0	801
174	5	3,607	−25.5	547
188	1	559	−20.9	546
188	2	3,023	21.5	397
188	3	6,782	−17.1	740
(*c*) Southern Pine				
289	1	1,321	29.1	203
289	2	—[a]	—[a]	—[a]
289	3	4,826	21.7	203
292	1	254	22.0	203
292	2	3,556	25.5	538
292	3	5,410	25.6	732
297	1	305	17.5	203
297	2	1,829	16.5	203
297	3	3,750	15.1	203

[a]Data lost due to a processing problem.

segment diameter, GTSTRUDL generates all nodes on the three concentric cylindrical surfaces necessary to create the element mesh for each segment. The element stiffness matrices were built using the E_L and predicted E_R, E_T, G, and ν. Such factors as spiral grain and element position in the cross section were taken into account. When knots were present in a segment, the elastic properties (previously assigned) for the elements were replaced to include the knot effect on the central element and the associated grain deviation on neighboring elements using the algorithm described previously. The loading was applied at the end of the segment using the GTSTRUDL boundary conditions statements.

TABLE 4. Evaluation of Proportional Factor between Wood Strength and Stress for 4,448-N Load

Pole segment (1)	Location above ground line (mm) (2)	Maximum stress (MPa) (3)	Modulus of rupture (MPa) (4)	Proportional factor (5)
(*a*) Western Red Cedar				
85-1	152	11.2	56.7	5.06
85-2	3,581	12.9	61.2	4.75
85-3	5,893	15.2	63.0	4.14[a]
85-4	6,731	12.0	62.4	5.20
88-1	660	6.9	55.3	8.06
88-2	2,413	8.4	53.3	6.32[a]
88-3	5,893	7.2	52.2	7.29
91-1	660	17.4	78.1	4.49
91-2	1,473	18.6	74.2	3.98[a]
91-3	2,413	17.0	70.7	4.17
(*b*) Douglas Fir				
162-1	864	20.0	69.6	3.48[a]
162-2	1,499	18.9	69.7	3.68
162-3	2,235	19.1	69.9	3.67
174-1	152	20.7	67.0	3.24
174-2	711	22.9	67.9	2.96
174-3	1,600	21.7	69.3	3.19
174-4	2,438	21.0	70.5	3.37
174-5	3,607	25.5	70.9	2.78[a]
188-1	559	21.0	89.7	4.28
188-2	3,022	21.5	77.6	3.62[a]
188-3	6,782	17.1	72.0	4.23
(*c*) Southern Pine				
289-1	1,321	29.1	52.7	1.80[a]
289-2	—[b]	—[b]	—[b]	—[b]
289-3	4,826	21.7	53.5	2.46
292-1	254	22.0	41.9	1.91
292-2	3,556	25.5	47.7	1.87
292-3	5,410	25.6	46.2	1.80[a]
297-1	305	17.5	55.0	3.14
297-2	686	16.5	49.5	3.00[a]
297-3	3,810	15.1	46.1	3.06

[a]Controlling ratio.
[b]Data lost due to processing problem.

The mesh created for the model was fitted over the segment chosen and oriented such that the four central disks (30.5 cm [12 in.] of the segment) contained the most critical knots. This was done to avoid the effect of boundary conditions on the first disk and loading on the last disk. For each segment selected, the location, geometric characteristics, spiral grain, and elastic properties were determined using straight-line interpolation (Fig. 7). After the input file was built, the program was executed.

TABLE 5. Strength versus Actual Values for Pole Strength and Failure Location

Pole number (1)	Predicted pole strength (kN) (2)	Actual pole strength (kN) (3)	Difference (%) (4)	Predicted[a] failure location (mm) (5)	Actual failure location (mm) (6)
(*a*) Western Red Cedar					
85	14.0	12.6	10.8	6,248	6,980
88	19.8	19.9	−0.5	2,743	2,621
91	13.2	14.2	−7.1	1,524	488
(*b*) Douglas Fir					
162	15.5	15.9	−2.8	1,128	1,006
174	12.4	12.4	0.0	3,810	3,962
188	16.1	17.0	−5.2	3,322	7,010
(*c*) Southern Pine					
289	8.0	9.6	−16.8	1,402	1,554
292	8.0	9.2	−13.1	5,669	5,639
297[b]	14.4	15.5	−7.3	396	610

[a]The predicted failure location was located the lowest stress/strength ratio occurred.
[b]Values adjusted using the revised small, clear specimen bending strength.

The results computed during the analysis were sent to an output file where the average element stresses, node displacements, and principal stresses were presented. Based on GTSTRUDL analysis of the 4,448-N (1-kip) load, the principal stresses were calculated. The maximum stress parallel to grain found in the segment was compared with the wood strength, as determined from tests on small clear specimens, to predict the pole strength.

The output for each segment analyzed by GTSTRUDL was scanned and the distribution of parallel to grain stresses in each of the seven disks observed. The maximum stress and corresponding locations were determined in the sections. Twenty-nine segments were subjected to the finite element analysis. Table 3 summarizes the results of the analyses, only the observed maximum stress parallel to grain due to the applied load (generated by the 4,448-N [1-kip] load) in each pole segment are presented.

Recognizing the variation in properties along the pole length, wood strength at each segment was computed. To predict the maximum load (strength) linear behavior was assumed for the stress-strain relationship, and a proportional factor between the wood strength and the stress generated by the 4,448-N (1-kip) load was computed for each segment. These factors, applied to the original load, led to the estimation of the pole strength. In Table 4, the proportional factor is presented for each segment and the maximum load obtained. The predicted strength was the least value found in Table 4. Pole-strength and failure location predictions as well as experimental results are presented in Table 5.

The criteria to predict the failure location were based on the combination of stress parallel to grain due to the applied load and the wood strength determined from tests on small, clear specimens. Figs. 8–10 show where the maximum stresses occurred on each pole, and the underlined segments illustrate where the ratio of parallel to grain stress to wood strength was

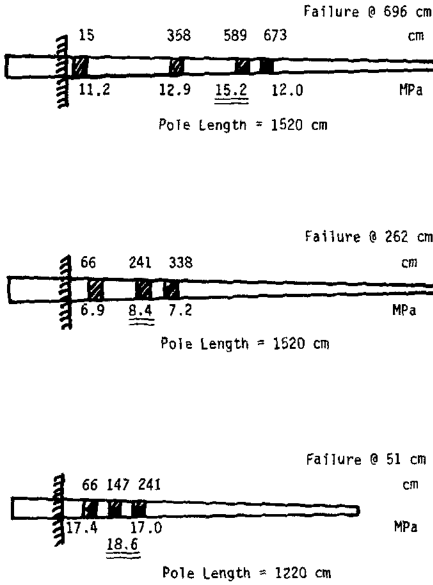

FIG. 8. Failure Locations and Maximum Stresses on Western Red Cedar Poles

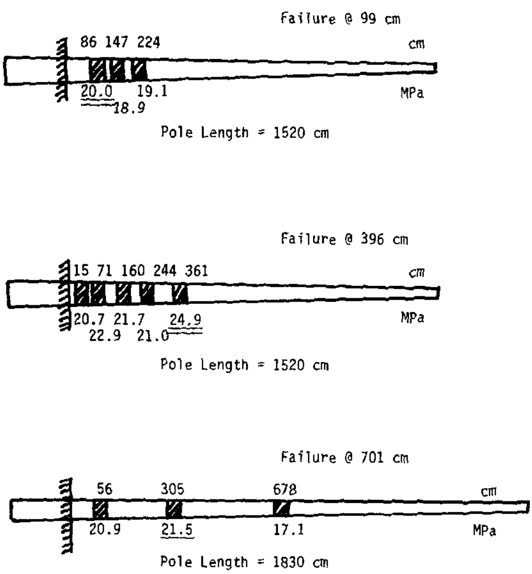

FIG. 9. Failure Locations and Maximum Stresses on Douglas Fir Poles

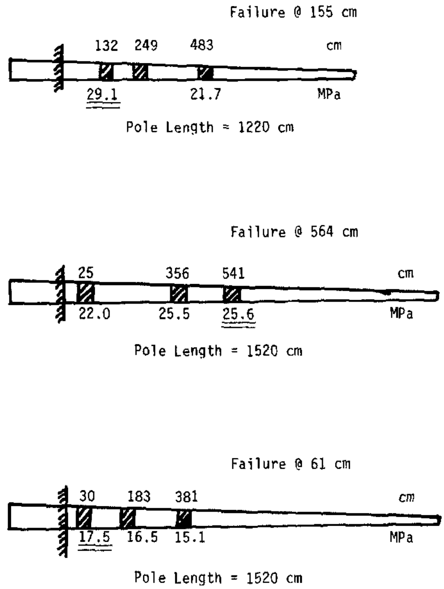

FIG. 10. Failure Locations and Maximum Stresses on Southern Pine Poles

a minimum. Table 5 includes the distance from the ground line where failure was predicted for each pole.

RESULTS

Figs. 8–10 illustrate the actual and predicted locations of failure and theoretical stress levels. From these figures and data in Table 5, it can be seen that the correct failure location was predicted in six of nine poles. Furthermore, the difference between experimental and predicted results ranged between −16.8% and 10.8% with an average difference of −7%. Since only three poles were tested for each species, the data were not sufficiently sensitive to determine any species effect. In all but one pole, the predicted strength was less than the experimental value. This suggests a conservative tendency of the model.

ANALYSIS

Grain deviation due to spiral grain or local deviation associated with knots may influence pole strength. Traditional methods of predicting pole strength are based on extrapolation from tests on small, clear specimens. In an attempt to improve on this crude method, empirical and 2-D numerical models have been developed. Predictions from these models lacked the accuracy and sensitivity to pole characteristics necessary to be generally useful.

The study described here was based on the assumption that a 3-D modeling of a pole was a rational characterization of the actual pole geometry. The model is able to account for spiral grain and pole inhomogeneity in a most rational way. The more complicated issue of knots and their associated grain deviation are handled through a theoretical flow-grain model and empirical consideration of knot properties.

The prediction of failure location in two-thirds of the poles suggests that, from a visual examination of the pole surface, a considerable degree of failure location variability can be accounted for. Furthermore, the prediction of the strength to within about 7% on average is a considerable improvement over techniques currently used. Therefore, it is rational to conjecture that the model represents a tool useful in realizing more rational pole grading procedures.

Since only three poles from each of the three species was studied, the data presented in Table 5 were insufficiently sensitive to generalize about species effects.

CONCLUSIONS

A technique was developed to model the growth characteristics, including knots, spiral grain, and variation of basic wood properties (bending stiffness and strength), using a 3-D finite element methodology. Analyses performed on the more critical segments along the pole length (as determined by a visual inspection) proved to be very successful and showed a vast improvement over the 2-D approach. Model verification was obtained using data collected from tests of full-size poles from three wood species.

For the nine poles studied, the predicted values for strength differed from experimental results by between -16.8% and 10.8%, with an average deviation of -7%. With regard to the prediction of failure location, in two-thirds of the cases (six of nine poles), the actual failures occurred at the predicted points. In these cases, knots were observed to be present in the segments. In the remaining one-third of the cases (three poles), the failure mechanisms were missed and rupture occurred in different locations. The failure mechanism in these cases was influenced by some phenomenon, or internal characteristic, not recognizable from a visual inspection of the pole surface.

From the results of this study, it is clear that the viability of a 3-D approach to pole-strength and failure location prediction is demonstrated, though the process is not without limitations. Growth characteristics on the poles were observed by visual inspection of the pole surface, and the modeled segments were located where occurrence of such growth characteristics was judged to be the most critical. As such, this model can be useful in modernizing grading procedures. However, pole characteristics that can not be determined from a surface inspection may severely influence mechanical behavior. Therefore, a more complete model is necessary if improved results are sought.

APPENDIX. REFERENCES

Annual book of ASTM standards 04.09 Wood, D-143. (1988). ASTM, Philadelphia, Pa.

Bodig, J. (1986). "Effect of knots on pole strength." *Final Report WSL-5*, Western Wood Preservers Inst., Fort Collins, Colo.

Bodig, J., and Goodman, J. R. (1973). "Prediction of elastic parameters for wood." *Wood Sci.*, 5(4), 249–264.

Cramer, S. M. (1981). "A stress analysis model for wood structural members," MS thesis, Colorado State University, Fort Collins, Colo.

Cramer, S. M., and Goodman, J. R. (1986). "Failure modeling: A basis for strength prediction of lumber." *Wood and Fiber Sci.*, 18(3), 446–459.

Cramer, S. M., and McDonald, K. A. (1989). "Predicting lumber tensile stiffness and strength with local grain angle measurements and failure analysis." *Wood and Fiber Sci.*, 21(4), 393–410.
Dabholkar, A. (1980). "Finite element analysis of wood with knots and cross grain," PhD dissertation, Colorado State University, Fort Collins, Colo.
Dashiell, J. A. (1985). "Effect of growth characteristics on the bending strength of wood poles," MS thesis, Colorado State University, Fort Collins, Colo.
Goodman, J. R., Vanderbilt, M. D., Criswell, M. E., and Bodig, J. (1981). "Probability-based design of wood transmission structures." *Analysis and probability-based design of wood utility structures (EL-2040)*, vol. 2, Electric Power Res. Inst., Palo Alto, Calif.
GTSTRUDL user's manual. (1985). Georgia Inst. of Tech., Atlanta, Ga.
Johnson, R. A., and Galligan, W. L. (1983). "Estimating the concomitance of lumber strength properties." *Wood and Fiber Sci.*, 15(3), 235–244.
Milne-Thompson, L. M. (1950). *Theoretical hydrodynamics*. The MacMillan Co., New York, N.Y.
Pellicane, P. J. (1983). "A sampling strategy useful in full-distribution simulation." *Wood Sci. and Tech.*, 17(4), 279–283.
Pellicane, P. J. (1984). "Application of the S_B distribution to the simulation of correlation lumber properties data." *Wood Sci. and Tech.*, 18(2), 147–156.
Pellicane, P. J. (1985). "Goodness-of-fit analysis for lumber data." *Wood Sci. and Tech.*, 19(2), 117–129.
Pellicane, P. J. (1993). "Application of the S_B distribution to the prediction of concomitant wood properties." *Wood Sci. and Tech.*, 27(2), 97–108.
Phillips, G. E., Bodig, J., and Goodman, J. R. (1981). "Flow grain analogy." *Wood Sci.*, 14(2), 55–64.
Tichy, R. J. (1983). "Concomitant strength relationship for lumber." *J. Struct. Engrg.*, ASCE, 109(8), 1854–1868.
Wang, Y. (1987). "Stress grading of utility poles," PhD dissertation, Colorado State University, Fort Collins, Colo.
Wood, L. W., and Markwardt, L. J. (1965). "Derivation of fiber stress values of wood poles." *Forest Products Lab. Res. Paper No. 39*, U.S. Forest Service, U.S. Dept. of Agric., Madison, Wis.
Zandbergs, J. G., and Smith, F. W. (1988). "Finite element fracture prediction for wood with knots and cross grain." *Wood and Fiber Sci.*, 20(1), 97–106.